Assembly of Major Histocompatability Complex (MHC) Class II Transcription Factors: Association and Promoter Recognition of RFX Proteins

Amy L. Burd, Richard H. Ingraham, Susan E. Goldrick, Rachel R. Kroe, James J. Crute,‡ and Christine A. Grygon*,‡

Department of Immunology and Inflammation, Boehringer Ingelheim Pharmaceuticals, Inc., 900 Ridgebury Road, Post Office Box 368, Ridgefield, Connecticut 06877-0368

Received December 22, 2003; Revised Manuscript Received April 16, 2004

ABSTRACT: Major histocompatibility complex (MHC) class II genes are regulated at the transcriptional level by coordinate action of a limited number of transcription factors that include regulatory factor X (RFX), class II transcriptional activator (CIITA), nuclear factor Y (NF-Y), and cyclic AMP-response element binding protein (CREB). Here, the MHC class-II-specific transcription factors and CREB were expressed in insect cells with recombinant baculoviruses, isolated, and characterized by biochemical and biophysical methods. Analytical ultracentrifugation (AUC) has demonstrated that RFX is a heterotrimer. A heterodimer of RFX5 and RFX-AP was also observed. A high-affinity interaction ($K_d = 25$ nM) between RFX5 and RFX-AP was measured by isothermal titration calorimetry (ITC), while the interaction between RFX-AP and RFX-ANK is at least an order of magnitude weaker. The biophysical data show that the interaction between RFX-AP and RFX5 is a key event in the assembly of the heterotrimer. Fluorescence anisotropy was used to determine protein−nucleic acid binding affinities for the RFX subunits and complexes binding to duplex DNA. The RFX5 subunit was found to drive recognition of the promoter, while the auxiliary RFX-AP and RFX-ANK subunits were shown to contribute to the specificity of binding for the overall complex. AUC experiments demonstrate that in the absence of additional subunits, monomeric RFX5 binds to X-box DNA with a 1:1 stoichiometry. Interactions between CREB, CIITA, and RFX in the absence of DNA were demonstrated using bead-based immunoprecipitation assays, confirming that preassociation with DNA is not required for forming the macromolecular assemblies that drive MHC class II gene expression.

Major histocompatibility complex (MHC)[1] class II molecules are heterodimeric surface proteins that are fundamental to the development and engagement of the immune system. In the thymus, MHC class II proteins effectively mold the T-cell repertoire through positive and negative selection by presenting autoantigens to developing CD4+ T cells. This induces CD4+ T cells that harbor autoreactive T-cell receptors (TCRs) to enter the apoptotic pathway and non-autoreactive cells to develop into mature CD4+ T cells capable of engaging in an immune response (*1*, *2*).

In the periphery under normal conditions, MHC class II molecules are expressed on antigen-presenting cells (APCs), specifically B cells, macrophages, and dendritic cells. These cells process extracellular antigens and present them on their cell surfaces complexed with MHC class II molecules. Recognition of antigen by CD4+ T cells and the engagement of MHC class II molecules with TCRs initiate a signaling process that leads to T-cell activation, expansion, and expression of soluble cytokines and membrane-bound co-stimulator molecules. These functions are essential for effectively clearing the majority of bacterial and fungal infections.

MHC class II molecules have also been found to play a central role in the development of autoimmune diseases, including rheumatoid arthritis, multiple sclerosis, systemic lupus erythematosus, and insulin-dependent diabetes mellitus. In these conditions, initial tissue destruction and inflammation fuels MHC class-II-mediated antigen presentation, resulting in the engagement of autoreactive T cells and ultimately leading to clinical disease. Thus, the regulated expression of MHC class II molecules is of central importance in balancing immune responses against foreign pathogens and autoantigens (*3*).

Genetic characterization of patients with bare lymphocyte syndrome (BLS) has resulted in the identification of four genes whose protein products appear solely to participate in the regulation of MHC class II expression. BLS is characterized by a loss of MHC class II expression resulting from mutations or defects in the transcription factors that mediate

* To whom correspondence should be addressed. Phone: (203) 798-5651. Fax: (203) 837-5651. E-mail: cgrygon@rdg.boehringer-ingelheim.com.

‡ These authors contributed equally to this work.

[1] Abbreviations: MHC, major histocompatibility complex; RFX, regulatory factor X; CIITA, class II transcriptional activator; NF-Y, nuclear factor Y; CREB, cyclic AMP-response element binding protein; AUC, analytical ultracentrifugation; TCR, T-cell receptor; BLS, bare lymphocyte syndrome; APC, antigen-presenting cell; PCR, polymerase chain reaction; HEPES, [4-(2-hydroxyethyl)piperazine-1-ethanesulfonic acid]; DTT, dithiothreitol; PMSF, phenyl-methylsulfonyl-fluoride; TRIS, *N*-tris-(hydroxymethyl)aminomethane; EDTA, ethylenediaminetetraacetic acid; TES, (*N*-tris[hydroxymethyl]methyl-2-aminoethanesulfonic acid); CHAPS, {3-[(3-cholamidopropyl)dimethylammonio]-1-propanesulfonate}; EGTA, ethyleneglycol-bis-(β-aminoethyl ether) *N*,*N*,*N*′,*N*′-tetraacetic acid; TCEP, tris(2-carboxyethyl) phosphine hydrochloride; MALDI/TOF, matrix-assisted laser desorption/time of flight; ITC, isothermal titration calorimetry.

10.1021/bi030262o CCC: $27.50
Published on Web 09/21/2004

transcription of these genes (*4*, *5*). There are four BLS complementation groups (A, B, C, and D) that have been defined by genetic defects in four different proteins required for MHC class II transcription (*6*). Complementation group A is defined by molecular defects that reside in the gene encoding class II transcriptional activator, CIITA (*7*). Patients in complementation groups B, C, and D are characterized by mutations within the heterotrimeric DNA-binding protein, regulatory factor X (RFX) (*8*−*12*). RFX is a ubiquitously expressed multimeric DNA-binding complex comprised of three subunits RFX5 (*9*), RFX-AP (*10*), and RFX-ANK (*11*−*12*).

MHC class II promoters contain four cis-acting sequences identified as the W (or S), X1, X2, and Y boxes (*6*). The RFX complex binds to the X1 box of the promoter (*13*). Two other general transcription factors, cyclic AMP response element binding protein (CREB) and nuclear factor Y (NF-Y), bind to the X2 and Y boxes, respectively (*14*−*18*). Because the spacing between the conserved sequences cannot be altered, cooperative interactions between RFX, CREB, and NF-Y have been postulated to account for the stable assembly of the higher order nucleoprotein complex or enhanceosome, essential for activation of the promoter (*19*−*23*). Further regulation of promoter activity is accomplished by CIITA (*7*, *24*−*25*), which does not bind DNA on its own, but has been shown to interact with factors on the MHC class II promoter (*26*−*28*). CIITA functions as a molecular switch that controls the cell type specificity of MHC class II expression, restricting constitutive expression to professional APCs and regulating inducible expression in other cell types when the IFN-γ signaling pathway is engaged (*7*, *24*−*25*, *29*−*31*).

Our understanding of the details surrounding the assembly of the transcription factors that regulate MHC class II gene transcription has increased significantly through studies that have primarily relied upon extracts or partially purified material from MHC class II positive cells and transiently expressed materials. Additional insights and greater quantitative understanding of the forces that drive transcription factor assembly can be gained using both biophysical and biochemical approaches of highly defined systems. In this report, the individual subunits of RFX and interacting partners CREB and CIITA were expressed in insect cells with recombinant baculovirus vectors. Rapid isolation schemes were developed for the individual subunits and assemblies of RFX along with the CREB and CIITA proteins. Biochemical and biophysical methods were used to characterize the purified transcription factors and their ability to interact with each other and artificially assembled MHC class II promoter elements. Our findings indicate that the RFX5 subunit drives recognition of class II promoter elements and that preassociation with DNA is not required for forming the macromolecular assemblies that drive MHC class II gene expression.

MATERIALS AND METHODS

Plasmids and Viruses. Baculovirus transfer vectors were made for RFX5 (accession number X85786), RFX-AP (accession number Y12812), RFX-ANK (accession number AF094760), CREB (accession number 117434), and CIITA by PCR-based cloning methods, unless otherwise noted. Open-reading frames that encoded the three subunits of RFX and CREB were made by the PCR amplification of a stimulated lymphocyte cDNA library with primer pairs RFX5 (F), 5′-CCCGGGTACCTTCTAGATATGGCAGAAGATGAGCCTGATGCTAAGAGCCC-3′; RFX5 (R), 5′-GCGGCCGCTTATCATGGGGGTGTTGCTTTTGGGTCTTTATGCTCCTGGG-3′; RFX-AP (F), 5′-GGGGTCGTGGACCCCGGCCAGGTCTTAGCAGC-3′; RFX-AP (R), 5′-ATAAAAACCATGTAGATGTTCTTGGTAAGTTCCC-3′; RFX-ANK (F), 5′-GGGGGGACAGAGGAGGCTCGTGGGGAGCTTTCCCC-3′; RFX-ANK (R), 5′-TGTTCCCTGAGTGTCTGAGTCCCCGGCAGGCGGCC-3′; and CREB (F), 5′-GGGATCCATGACCATGGAATCTGGAGCC-3′; CREB (R), 5′-GCGGCCGCTTATTAATCTGATTTGTGGCAGTAAAG-3′ and inserted into pCR2.1 to create pCR2.1/RFX5, pCR2.1/RFX-AP, pCR2.1/RFX-ANK, and pCR2.1/CREB, respectively. On confirmation of the sequence, a second set of PCRs were performed with the pCR2.1/RFX-AP and pCR2.1/RFX-ANK plasmids and primer sets RFX-AP (exp F), 5′CCCGGATCCATGGAGGCGCAGGGTGTAGCGGAGGGC-3′ with RFX-AP (exp R), 5′-CCGGGAATTCTTATCACATTGATGTTCCTGGAAACTGCTG-3′; and RFX-ANK (exp F), 5′-CCCGGATCCATGGAGCTTACCCAGCCTGCAGAAGACC-3′ with RFX-ANK (exp R), 5′-CCGGGAATTCTTATCACTCAGGGTCAGCGGGCACCAGGTTCG-3′, respectively. The PCR products were cloned into the pCR2.1 vector and sequence-verified. Baculovirus transfer vectors were made for RFX-AP, RFX-ANK, and CREB by using introduced 5′ *Bam*H1 and 3′ *Not*I sites to create pVL1393/RFX-AP, pVL1393/RFX-ANK, and pVL1393/CREB, respectively. The pCR2.1/RFX5 sequence was inserted into pVL1393 with the introduced 5′ *Xba*I and 3′ *Not*I sites to make pVL1393/RFX5.

The RFX-AP sequence was fused to the CA21 epitope (SKRSMNDPY) coding sequence by the introduction of a *Nhe*I site in place of the RFX-AP terminator codon and subcloning into a pVL1393-derived plasmid provided by Dr. Steven Pullen (Boehringer-Ingelheim Pharmaceuticals, Inc.). The RFX-AP open-reading frame was PCR-amplified from pCR2.1/RFX-AP with the primer pair RFX-AP (exp F) and RFX-AP (R, *NheI*), 5′-GCTAGCTTATCACATTGATGTCCTGGA-3′, subcloned into pCR2.1, sequence confirmed, and subcloned into the CA21 epitope-encoding plasmid to make pVL1393/RFX-AP-CA21. The FLAG epitope was introduced into the RFX-ANK sequence by subcloning the RFX-ANK sequence from pVL1393/RFX-ANK with *Nco*I and *Not*I restriction endonuclease sites and insertion into pFlag/1393 (*32*) to make pVL1393/FLAG-RFX-ANK. The plasmid pcDNA2.FLAG.CIITA8 (*33*) was obtained from Jenny Ting (Lineberger Comprehensive Cancer Center, University of North Carolina at Chapel Hill, NC). The FLAG-CIITA sequence was subcloned into pVL1393 using the flanking *Eco*RI sites to make pVL1393/FLAG-CIITA. The orientation of the transfer vector insert was confirmed by DNA sequencing.

Each of the above baculovirus transfer vectors were recombined into BaculoGold baculovirus DNA with standard methods and high titer recombinant virus stocks generated. This produced the baculoviruses AcMNPV/RFX5, AcMNPV/RFX-AP, AcMNPV/RFX-ANK, AcMNPV/CREB, AcMNPV/RFX-AP-CA21, AcMNPV/FLAG-RFX-ANK, and AcMNPV/FLAG-CIITA. These vectors expressed high levels

of the RFX5, RFX-AP, RFX-ANK, CREB, RFX-AP-CA21, FLAG-RFX-ANK, and FLAG-CIITA proteins, respectively.

Buffers. Buffer A was 20 mM HEPES at pH 7.5, 1.0 mM DTT, 10 mM sodium metabisulfite, 10 μg mL^{-1} leupeptin, 10 μg mL^{-1} pepstatin A, and 1.0 mM PMSF. Buffer B was 20 mM HEPES at pH 7.5, 10% (v/v) glycerol, 1.0 mM DTT, 0.1 mM EDTA, 0.1 mM EGTA, and 1.0 mM PMSF. Buffer C was buffer A with the addition of 10% sucrose and 2 M NaCl. Buffer D was 10 mM TRIS-HCl at pH 7.5, 80 mM NaCl, and 1.0 mM EDTA. Buffer E was 12 mM HEPES at pH 7.5, 12% (v/v) glycerol, 150 mM NaCl, 3.0 mM $MgCl_2$, and 0.3 mM DTT. Buffer F was 20 mM HEPES at pH 7.5, 0.1% NP40, 100 mM NaCl, 1.0 mM $MgCl_2$, and 1.0 mM DTT. Buffer G was 20 mM TES at pH 7.0, 200 mM NaCl, 0.05% CHAPS, and 1 mM DTT. Buffer H was 20 mM TES at pH 7.0, 150 mM KCl, 12% glycerol, 3 mM $MgCl_2$, 0.05% CHAPS, and 1 mM TCEP.

Insect Cell Growth, Use of Recombinant Baculoviruses, and Preparation of Cell Extracts. Spodoptera frugiperda (Sf21) cells were maintained and infected as described previously using media supplemented with 5% fetal bovine serum (HyClone). For the expression of the RFX, CIITA, or CREB proteins, insect cells were singly or multiply infected and harvested 3 days postinfection, and nuclear and cytosolic fractions were prepared as previously described (*34*). On harvesting of the infected Sf21 cells, all subsequent isolation procedures were performed at 4 °C or on ice. The cytosolic fractions were clarified prior to use by centrifugation at 120000*g* for 75 min. Nuclear fractions were resuspended in an equal volume of buffer A with 10% (w/v) added sucrose. The nuclear fraction was salt-extracted by rapid mixing with an equal volume of buffer C followed by incubation on ice for 10 min and centrifugation at 440000*g* for 8 min.

Chromatography Media and Columns. SOURCE 15S, SOURCE 15Q, heparin agarose, and a prepacked column of Sephacryl S-300HR were from Amersham Pharmacia BioTech. Prepacked BioScale DEAE columns were from BioRad. Anti-FLAG M2 agarose and FLAG peptide were from SIGMA.

Isolation of Recombinant RFX, RFX Subunits and Subassemblies, FLAG-CIITA, and CREB Proteins. Methods were developed to isolate RFX, subassemblies of RFX containing RFX5 and RFX-AP or RFX5 and RFX-ANK proteins, or separate RFX proteins. RFX5, the subassembly of RFX5/RFX-AP, and the trimeric complex of RFX were isolated from high-salt extracts of the nuclear fraction of baculovirus-infected Sf21 cells. Recombinant proteins were precipitated by the addition of 40% v/v of a saturated ammonium sulfate solution. Precipitated proteins were resuspended in buffer B with 200 mM NaCl. The samples were diluted with buffer B to a conductivity corresponding to a NaCl concentration of 150 mM, further clarified by ultracentrifugation, and chromatographed through a SOURCE 15S column. Proteins were eluted with a 150 mM to 2 M NaCl gradient.

RFX-AP and RFX-AP-CA21 proteins were isolated from ammonium-sulfate-precipitated cytosolic extracts of baculovirus-infected Sf21 cells followed by ion-exchange chromatography. Recombinant proteins were precipitated by the addition of 60% v/v of a saturated ammonium sulfate solution. Precipitated proteins were resuspended in buffer B containing 200 mM NaCl. The ionic strength of the samples was adjusted by dilution with buffer B to a conductivity corresponding to a solution containing 100 mM NaCl, clarified by ultracentrifugation, and chromatographed through a SOURCE 15Q column. Proteins were eluted with a 100 mM to 2 M NaCl gradient. RFX-ANK was isolated as described above for the RFX-AP proteins, except that the resuspended ammonium sulfate precipitate was diluted to an ionic strength corresponding to 200 mM NaCl prior to chromatography. Peak fractions containing the RFX-ANK protein were further chromatographed through a BioScale DEAE column. Proteins were eluted with a 200 mM to 2 M NaCl gradient. The FLAG-RFX-ANK protein was isolated by immunoaffinity chromatography using an anti-FLAG M2 Sepharose column. Cytosolic extracts were applied to an anti-FLAG M2 Sepharose column, and after washing with buffer B containing 400 mM NaCl, the FLAG-RFX-ANK protein was eluted in buffer B containing 150 mM NaCl and 250 μg mL^{-1} FLAG peptide.

FLAG-CIITA was isolated from cytosolic extracts of baculovirus-infected Sf21 cells. The recombinant protein was precipitated by the addition of 20% v/v of a saturated ammonium sulfate solution. Precipitated proteins were resuspended in buffer B containing 200 mM NaCl. The conductivity of the sample was adjusted to correspond to a solution of 100 mM NaCl and chromatographed through a heparin agarose column. Proteins were eluted with a 100 mM to 2 M NaCl gradient. CREB was isolated from nuclear extracts of baculovirus-infected Sf21 cells. The recombinant protein was precipitated as described for FLAG-CIITA, resuspended in buffer B with 200 mM NaCl, and isolated as outlined for RFX-ANK by chromatography through SOURCE 15S and BioScale DEAE.

Typical yields from 40 g of starting insect cell paste containing recombinant RFX, RFX5/RFX-AP subassembly, and RFX5, were 10, 34, and 16 mg, respectively. The identity of the individual proteins was confirmed by matrix-assisted laser desorption/time-of-flight (MALDI/TOF) mass spectrometry. The concentrations of purified proteins were determined as described (*35*), frozen under liquid N_2, and stored at −80 °C until use.

DNA Substrates for Monitoring Protein−Nucleic Acid Interactions. DNA molecules used for measuring RFX nucleic acid interactions were from the Midland Certified Reagent Company or IDT and purified by polyacrylamide gel electrophoresis. The oligonucleotides were resuspended, and concentrations were determined by UV absorbance values and calculated molar extinction coefficients (*35*). Double-stranded DNA probes were hybridized by mixing complementary strands, designated F for forward or top and R for reverse or bottom, in equimolar amounts in buffer D. Mixtures were then heated to 95 °C and cooled to room temperature over a period of several hours. The sequences of DNA substrates were as follows: DRA 32-mer X-box mimic (F), 5′-CCCF*CCCTTCCCCTAGCAACAGATGCGTCATC-3′; DRA 32-mer X-box mimic (R), 5′-GATGACGCATCTGTTGCTAGGGGAAGGGGGGG-3′; DRA 57-mer W/X-box mimic (F), 5′-GTCCTGGACCCTTTGCAAGAACCCTTCCCCTAGCAACAGATGCGTCATCTCAAAATA-3′; DRA 57-mer W/X-box mimic (R), 5′-TATTTTGAGATGACGCATCTGTTGCTAGGGGAAGGGTTCTTGCAAAGGGTCCAGGAC-3′; DRA 29-mer W-box mimic (F), 5′-CCCF*TCCTGGACCTTTGCAAGAACCCTTC-3′; DRA

29-mer W-box mimic (R), 5′-GAAGGGTTCTTGCAAAG-GTCCAGGAGGGG-3′; 28-mer dA·dT (F), 5′-AAAAAAAA-AAAAAAAAAAAAAAAAAAAA-3′; 28-mer dA·dT (R), 5′-TTTTTTTTTTTTTTTTTTTTTTTTTTTT-3′. DRA X and DRA W forward oligos were labeled with fluorescein as designated in the sequences above (F*).

Steady-State Fluorescence Anisotropy. Steady-state anisotropy measurements were made on an SLM 8100 Spectrofluorometer equipped with a thermostated sample chamber and Glan−Thompson polarizers. All measurements were made at 21.5 °C in 1-cm fluorescence cuvettes. Affinity constants for DNA−protein interactions were determined by titrating RFX, RFX subassemblies, or single subunits into a solution containing 20 nM DNA in buffer E. The excitation wavelength was 490 nm; fluorescence emission was detected through an LG-530 filter from Corion. The *g* factor was determined for each measurement. The anisotropy values used for data fitting were the average of 3−5 determinations. Total fluorescence intensity was also recorded. All data were analyzed using the SAS statistical software system (version 6.12, SAS Institute Incorporated, Cary, NC). The SAS MODEL procedure was applied to nonlinear models applying ordinary nonlinear least-squares regression techniques using the Marquardt−Levenberg minimization method (SAS-STAT Users Guide, version 6, 4th edition).

Size-Exclusion Chromatography (SEC). Protein samples for analytical ultracentrifugation analysis underwent additional fractionation using high-resolution SEC on an HP1090 HPLC with tandem Bio-Rad columns (Bio-Sil 400-5 in series with Bio-Sil 250) in buffer G. Apparent molecular weights were determined from sample elution volumes based on a calibration curve generated using the Bio-Rad gel-filtration standards consisting of thyroglobulin, bovine γ globulin, chicken ovalbumin, equine myoglobin, and vitamin B_{12}.

Analytical Ultracentrifugation. Experiments were performed using a Beckman Model XL-I analytical ultracentrifuge using either two sector (sedimentation velocity) or six-hole centerpieces (sedimentation equilibrium). Data for protein samples were collected at 230 nm. Data for the sedimentation velocity experiments of the RFX5/DNA complex were collected at both 280 and 260 nm. Sedimentation equilibrium experiments were performed in buffer G at 10 °C using rotor speeds of 9000, 12 000, 18 000, and 24 000 rpm at multiple concentrations as follows: RFX-AP, 8.13, 2.7, and 0.93 μM; FLAG-RFX-ANK, 10.5, 4.1, and 2.5 μM. Data were edited and analyzed using REEDIT and Win Non-Lin provided by the National Analytical Ultracentrifugation Facility at the University of Connecticut, Storrs, CT.

Sedimentation velocity analyses were performed at 50 000 rpm at 20 °C at the following concentrations: RFX5, 3.88 μM; RFX-AP, 12.95 μM; RFX-ANK, 4.4 μM; RFX5/RFX-AP, 1.68 μM; and RFX5/RFX-AP-CA21/FLAG-RFX-ANK, 0.85 μM.

Sedimentation velocity studies of the RFX5/DNA interaction were performed at 55 000 rpm at 20 °C in buffer H, using an unlabeled version of the X-box sequence noted above. Data were collected at 260 and 280 nm. Both RFX5 and X-box DNA were dialyzed against buffer H without prior SEC fractionation. The concentrations used for RFX5 and X-box DNA were 5 and 1 μM, respectively, both for the single component samples and for the mixture of RFX5 and DNA.

Global fitting of all of the sedimentation velocity data was performed using Sedfit version 8.4 written by Dr. Peter Schuck (*36*). Predicted partial specific volumes (ν), hydration parameters (δ), and protein extinction coefficients were calculated based on their amino acid composition using Sednterp version 1.07 (*37*). Calculations for shape analysis were performed using Sednterp version 1.07. Solvent density (ρ) and viscosity (η) were calculated using Sednterp version 1.07 based on the buffer composition.

ITC. The ITC experiments were performed using a Microcal VP-ITC (Northampton, MA). All proteins were dialyzed overnight at 4 °C prior to performing the experiments. To measure binding of RFX5 to RFX-AP, the sample cell of the calorimeter was loaded with 5 μM RFX5 in buffer E with 0.3 mM TCEP instead of DTT. The syringe was loaded with 74 μM RFX-AP in the same buffer. All solutions were degassed for 8 min. Titrations were performed at 25 °C. After completion of the titrations, baselines were manually drawn and subtracted from the data. The data were zeroed assuming the final injections of each titration represent only the heat of dilution. Data were fit using a one-site binding model available in the Origin ITC data analysis software (version 5.0).

Immunoprecipitation Assays. For immunoprecipitation studies, equimolar amounts (250 pmol) of isolated RFX5, RFX-AP-CA21, and FLAG-RFX-ANK were incubated at 25 °C for 15 min in buffer F. Anti-CA21 or anti-FLAG M2 Sepharose beads were added to the protein mixtures and incubated for an additional 1 h at 4 °C with constant inversion. The beads were washed 3 times with buffer F, and interacting proteins were detected by Western blotting. Samples were heated to 95 °C in SDS−PAGE loading buffer (3× red loading buffer with DTT, New England Biolabs), electrophoresed through a 12% TRIS-glycine polyacrylamide gel, and transferred to PVDF membranes. Membranes were blocked with TRIS-buffered saline containing 0.04% Tween 20 and 0.01% SDS with 3% bovine serum albumen for 1 h. RFX5 was detected with a rabbit polyclonal primary antibody conjugated to *N*-ethyl maleimide-activated ovalbumen. Detection of the bound primary antibody was with goat anti-rabbit antibody conjugated to horseradish peroxidase. RFX-AP-CA21 and FLAG-RFX-ANK were detected with biotinylated anti-CA21 and anti-FLAG M2 primary antibodies and a streptavidin conjugated to horseradish peroxidase secondary reagent. Detection of horseradish peroxidase was with 0.2 mg mL^{-1} 3-amino-9-ethyl-carbazole dissolved in 45 mM sodium acetate at pH 5.0 and 0.0072% H_2O_2. CIITA/RFX/CREB immunoprecipitation studies used equimolar amounts (250 pmol) of RFX, FLAG-CIITA, and CREB. The hybrid DRA W/X and dA·dT DNAs were added in various combinations and incubated with the proteins at 25 °C for 15 min. The complexes were adsorbed onto anti-CA21 Sepharose beads for 1 h, washed 3 times in buffer F, and analyzed by Western blotting as described above.

RESULTS

Expression and Isolation of RFX. To study the molecular mechanism(s) that promote RFX complex formation, recombinant baculoviruses expressing RFX5, RFX-AP, and

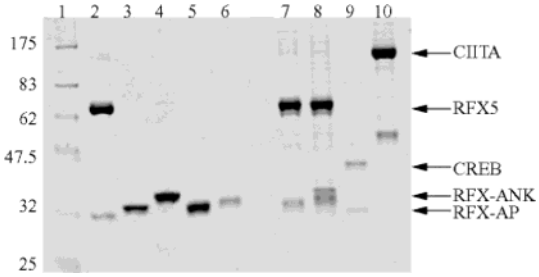

FIGURE 1: SDS−PAGE analysis of MHC class II transcription factors. Recombinant MHC class II transcription factors were expressed and isolated as described under the Materials and Methods. Lane 1 contained molecular mass markers. Lanes 2−10 contained 5 μg of RFX5, RFX-ANK, FLAG-RFX-ANK, RFX-AP, RFX-AP-CA21, RFX5/RFX-AP subassembly, RFX5/RFX-AP-CA21/FLAGRFX-ANK subassembly, CREB, and FLAG-CIITA, respectively. Proteins were analyzed by SDS−PAGE as outlined under the Materials and Methods and visualized by staining with Coomassie Brilliant Blue. Molecular mass markers are listed in kiloDaltons.

RFX-ANK were generated. Insect cells were either individually infected or co-infected with the RFX-expressing baculoviruses allowing for the isolation of RFX5, RFX-AP, RFX-ANK, RFX5/RFX-AP, and RFX5/RFX-AP/RFX-ANK (Figure 1). Isolation schemes were developed as described in the Materials and Methods and employed to generate proteins of sufficient quantity and purity for biochemical and biophysical analysis. Following isolation of the individual RFX proteins and assemblies, the identity of each protein and protein complex was confirmed by molecular weight determination using MALDI mass spectrometry (Table 1).

RFX Complex Is a Heterotrimer. Initial examination of the assembly of the RFX complex, trimeric complex, and subassemblies was accomplished by reconstituting equimolar amounts of the purified subunits. To simplify this analysis and enable coprecipitation studies from purified subunits, RFX-AP was engineered with a CA21 epitope at the C terminus (*32*) and RFX-ANK was engineered with a FLAG epitope at the N terminus. In coprecipitation experiments using anti-CA21 agarose beads, RFX-AP-CA21 was shown to interact with RFX5 (Figure 2). The weak interaction of FLAG-RFX-ANK and RFX-AP-CA21 was enhanced by RFX5. Multiple interactions within the RFX complex were also confirmed via coprecipitation experiments using anti-FLAG agarose beads, which demonstrated a direct association of RFX5 with FLAG-RFX-ANK. Again, the weak interaction of FLAG-RFX-ANK and RFX-AP-CA21 was enhanced through RFX5 association (Figure 2). None of the subunits interacted with the CA21 or FLAG epitopes alone (data not shown), demonstrating the specificity of the interactions. These data suggest that RFX5 drives the heteroassociation of the RFX complex allowing for multiple protein−protein interactions within the complex. Moreover, the interactions between RFX5 and either RFX-AP or RFX-ANK are stronger than the interaction between RFX-AP and RFX-ANK, because the amount of RFX-ANK precipitated with RFX-AP was negligible. Additionally, only the RFX5/RFX-AP subcomplex could be isolated from the reconstituted mixtures of recombinant proteins. The strengths of the interactions between RFX-ANK and either RFX5 or RFX-AP were insufficient to isolate either heterodimer from the reconstituted mixtures.

ITC was used to confirm the observation that RFX5 and RFX-AP form a tight complex. The results of this experiment (Figure 3) demonstrate that RFX5 and RFX-AP form a high-affinity complex with a 1:1 stoichiometry. The dissociation constant (K_d) for this interaction is 25 nM ($\Delta H = -3.3$ kcal/mol, $\Delta S = 24$ cal/mol K). In contrast, the dissociation constant for RFX-AP binding to RFX-ANK via ITC is at least an order of magnitude weaker (data not shown). These data, coupled with the above pull-down data, suggest that the nucleation event for RFX assembly is the association of RFX5 with RFX-AP. RFX-ANK then recognizes the RFX5/RFX-AP complex either through a new molecular surface created by the interface of the RFX5 and RFX-AP subunits or through a conformational change that exposes ankyrin recognition regions. These events are linked to the cooperative nature of RFX heterotrimer formation.

Biophysical characterization of the RFX proteins included SEC and analytical ultracentrifugation. On the basis of molecular weight protein standards, the individual subunits had apparent molecular weights of 471 000 (RFX5), 90 000 (RFX-AP), and 145 000 (RFX-ANK) (data not shown). The RFX complex of all three subunits eluted with an apparent molecular weight of 590 000 (data not shown). These values are all significantly larger than the predicted molecular weights for the monomers. This suggests that these proteins either exhibit significant asymmetry, self-association, non-specific column adsorption, or some combination of these factors. The peak shapes of the chromatograms provide additional insight into the quaternary structure of the proteins. Whereas the chromatograms of RFX-AP and RFX-ANK exhibited singlet peaks, those for RFX5 and complexes containing RFX5 exhibited three contiguous peaks, with the center peak being the largest. The multiplicity of peaks for samples containing RFX5 appears to be due to self-association. Some degree of aggregated material also appears to be present, eluting prior to the center peak. The amount of aggregation varied with the preparation but was generally observed to be less than 15%.

Sedimentation velocity experiments were conducted with the individual subunits and with selected complexes. Figure 4 displays $c(S)$ distribution plots for SEC-purified RFX5, RFX-AP, RFX-ANK, RFX5/RFX-AP, and RFX5/RFX-AP/RFX-ANK. It is clear from this figure that the purified subunits and complexes each sediment predominantly as one species. Table 1 summarizes both the sedimentation velocity and sedimentation equilibrium results for the proteins. The velocity data were analyzed with several different fitting algorithms using SedFit. The $S_{20,w}$ values for the primary species in each sample were first determined using the noninteracting discrete species model. The frictional coefficients (f/f_p) used for converting the S_{app} values obtained from the continuous $c(S)$ model to $S_{20,w}$ values were determined based on the noninteracting discrete species $S_{20,w}$ values using Sednterp. The results from both models yield nearly identical $S_{20,w}$ values for the various proteins and protein complexes (Table 1). The molecular weights determined using the continuous $c(M)$ distribution model also took into account the calculated frictional coefficients and are consistent with the masses expected for the monomers of the individual subunits and the heterodimer and heterotrimer for RFX5/RFX-AP and RFX, respectively.

Table 1: Biophysical Analyses of RFX

protein	M^a	$S_{20,w}{}^b$	f/f_p	prolate ellipsoid axial ratio (a/b)	$c(M)^c$	M_r (sed. equil.)^d
RFX5	65 205	3.76 (3.747−3.791) 3.79	1.524	5.92	64 600	
RFX-AP	28 396	1.88 (1.861−1.885) 1.85	1.826	10.51	27 100	31 800 (30 200−33 300)
RFX-ANK	28 143	2.06 (2.047−2.089) 2.16	1.509	6.81	27 700	29 700 (29 000−33 600)
RFX5/RFX-AP	65 377 28 364	4.39 (4.313−5.312) 4.40	1.681	8.19	94 400	
RFX	65 398 29 710 29 824	5.28 (5.261−5.304) 5.32	1.691	8.34	123 400	
DNA X-box mimic		3.02 (2.904−3.129) 3.05			21 800	20 400 (19 400−21 300)

[a] Molecular mass in Daltons as determined by MALDI mass spectrometry. [b] $S_{20,w}$, sedimentation constant at 20 °C in water. The upper values are calculated from the noninteracting discrete species models, and the lower values are calculated from the continuous $c(S)$ values. Values in brackets represent 68% confidence intervals. [c] Molecular mass in Daltons as determined by continuous $c(M)$ distribution model. [d] Weight-average molecular weight as determined by sedimentation equilibrium analysis using single-species fit as described under the Materials and Methods.

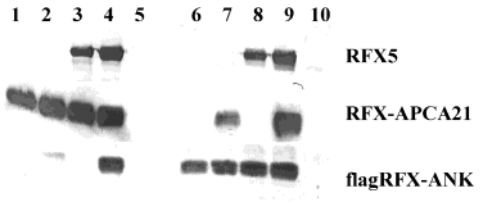

FIGURE 2: RFX subunit interactions. RFX and related subassemblies were reconstituted at a 1:1:1 ratio from isolated RFX5, RFX-AP-CA21, and FLAG-RFX-ANK proteins as outlined under the Materials and Methods. Anti-CA21 coprecipitations are shown in lanes 1−5. Lane 1, RFX-AP-CA21; lane 2, RFX-AP-CA21 + FLAG-RFX-ANK; lane 3, RFX-AP-CA21 + RFX5; lane 4, RFX-AP-CA21 + FLAG-RFX-ANK + RFX5; and lane 5, beads alone. Anti-FLAG coprecipitations are shown in lanes 6−9. Lane 6, FLAG-RFX-ANK; lane 7, FLAG-RFX-ANK + RFX-AP-CA21; lane 8, FLAG-RFX-ANK + RFX5; lane 9, FLAG-RFX-ANK + RFX-AP-CA21 + RFX5; and lane 10, beads alone.

Sedimentation velocity experiments provide information on both the shape and association state of proteins. Both RFX-AP and RFX-ANK sediment as monomers in the velocity studies. Modeling of the shapes of these two subunits as prolate ellipsoids suggests that they are asymmetric. This appears to be especially true for RFX-AP or complexes containing RFX-AP. The origin of this apparent asymmetry could arise from a number of factors including a loosely folded structure or a compact but asymmetric structure. These results are consistent with the observation that the apparent molecular weights as determined by SEC are much larger than the actual molecular weights. Binding of the RFX complex to its promoter may be facilitated by its extended asymmetric shape.

The sedimentation velocity analyses of RFX5 typically contain a small but measurable amount of dimer. Velocity studies of the various RFX complexes that contain RFX5 show that the RFX5 dimer is competent to bind both RFX-AP and RFX-ANK. To test the reversibility of the higher order forms of RFX association, additional velocity studies were performed with RFX5 alone. The percentage of monomer relative to dimer did not differ appreciably over a 3-fold concentration range, 5−15 μM, suggesting that the monomer and dimer were not in equilibrium during the course of the experiment (data not shown).

The results of the sedimentation equilibrium studies clearly demonstrate that both the RFX-AP and RFX-ANK subunits

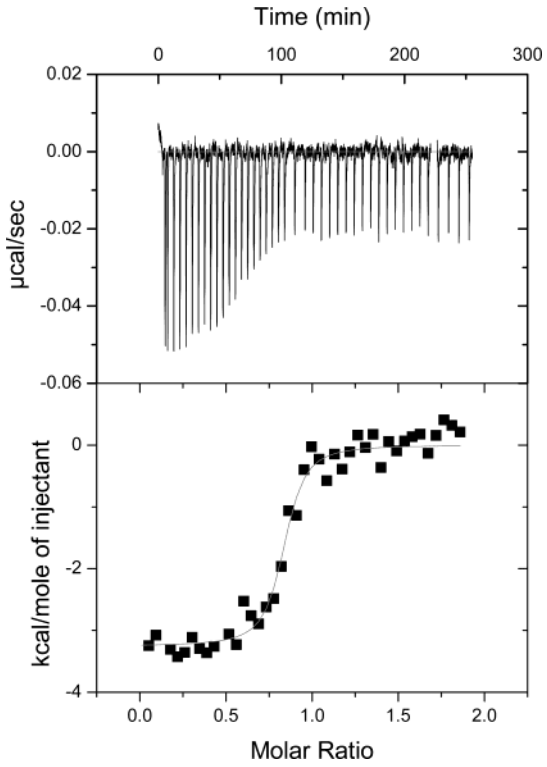

FIGURE 3: ITC. RFX-AP titrated into RFX5 measured at 25 °C.

are monomeric (Table 1). In contrast, when the data for RFX5 protein alone or in complex with the other subunits were analyzed using a single-species model, molecular weights significantly higher than those predicted for monomer, heterodimer, or heterotrimer, respectively, were obtained. Further diagnostic evaluation of the data indicated the formation of an aggregate during the course of the multiday sedimentation experiments as seen by a decrease in the average molecular weight as a function of the rotor speed. Hence, the data where RFX5 is present cannot be properly fit.

RFX5 Interacts with X-Box DNA as a Monomer. Sedimentation velocity studies of RFX5 in the presence and absence of X-box DNA were performed to examine the stoichiometry of the RFX5/DNA interaction. Data for these experiments were collected at both 260 and 280 nm. Collecting data at two wavelengths allowed for determination

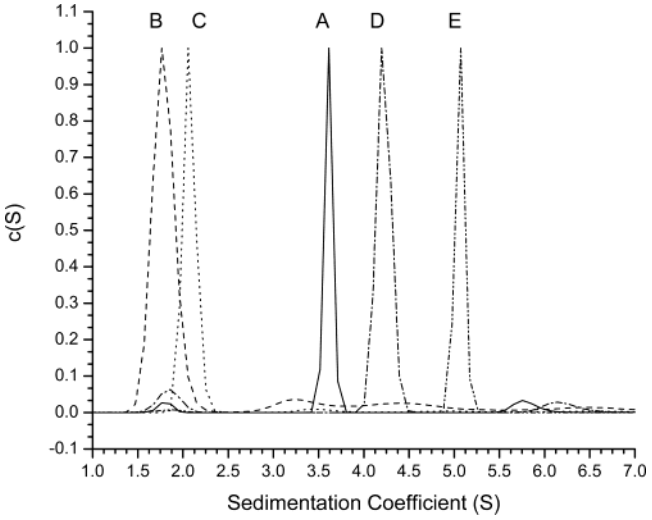

FIGURE 4: Sedimentation velocity $c(S)$ for RFX subunits and complexes. (A) RFX5, (B) RFX-AP, (C) RFX-ANK, (D) RFX5/RFX-AP, and (E) RFX.

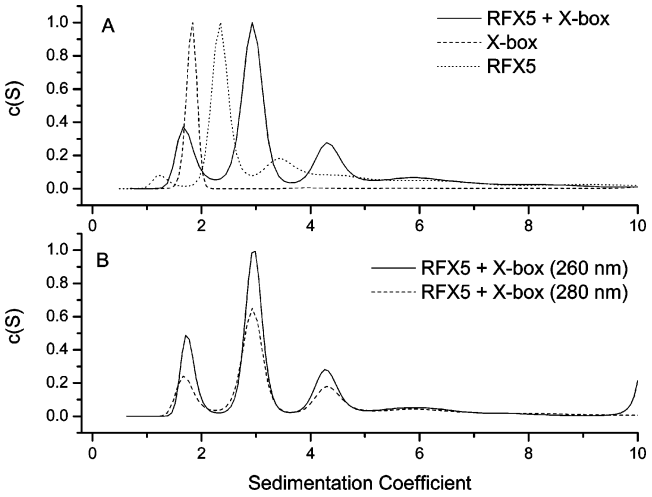

FIGURE 5: Sedimentation velocity $c(S)$ for RFX5 in the presence and absence of X-box DNA. (A) Data collected at 280 nm and normalized. RFX5 (···) sediments primarily as a monomer at 2.3 S_{app} with some dimer present at 3.4 S_{app}. X-box DNA (- - -) sediments as a monomer at 1.8 S_{app}. RFX5 + X-box DNA (—) sediments as a 1:1 complex at 2.9 S_{app} and as a 2:2 complex at 4.3 S_{app}. (B) RFX5 + X-box DNA data collected at 260 nm (—), and RFX5 + X-box DNA data collected at 280 nm (- - -). These data show that the ratio of protein−DNA in each of the complex species is identical.

of the ratio of DNA to protein present in each of the resolved species. These data show that RFX5 interacts with the X-box DNA with a 1:1 stoichiometry and that both the monomeric and dimeric forms of RFX5 are competent to bind DNA (Figure 5).

RFX5 Drives Sequence-Specific DNA Recognition. The binding affinities of the RFX subunits, subassemblies, and trimeric complex for DNA were determined using fluorescence anisotropy. For these experiments, a DNA sequence that mimics the X box of the HLA DRA promoter was labeled with fluorescein. Because fluorescence anisotropy is highly sensitive to changes in the molecular weight of the labeled species, binding of the RFX protein components is easily detected by an increase in the anisotropy signal (*38*). The magnitude of the anisotropy signal can be influenced by the asymmetrical shapes of the proteins as well as the

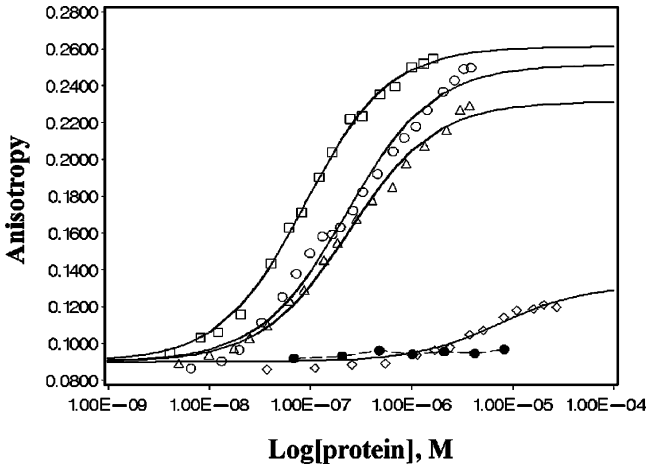

FIGURE 6: Binding of RFX proteins and subcomplexes to X-box DNA. DNA interaction assays were performed using fluorescence anisotropy as described under the Materials and Methods. The fluorescence anisotropy for RFX5 (○), RFX5/RFX-AP (□), RFX5/RFX-AP-CA21/FLAG-RFX-ANK (△), RFX-AP (◇), and RFX-ANK (●) was plotted as a function of the increasing protein concentration. Nonlinear regression analysis as described under the Materials and Methods converged to the following solution (where the value in parentheses is the standard error): RFX5, K_d = 199 (20) nM; RFX5/RFX-AP, K_d = 79 (4) nM; and RFX5/RFX-AP-CA21/FLAG-RFX-ANK, K_d = 193 (52) nM.

multimerization state. On the basis of the AUC data, the anisotropy data were fit to a single-binding site model for simplicity. As shown in Figure 6, it is not essential that all three subunits be present for DNA binding. RFX5 binds to the promoter sequence in the absence of the other RFX subunits (K_d = 198 ± 26 nM). The data suggest a weak interaction between RFX-AP and the X box; however, the relevance and nature of this interaction was not investigated further. RFX-ANK exhibited no detectable binding. To further examine the role of RFX-AP and RFX-ANK within the trimeric complex, the DNA binding of RFX5/RFX-AP (subcomplex) and the trimeric complex, RFX, were compared to RFX5 alone. The subcomplex of RFX5/RFX-AP had a slightly increased affinity (K_d = 76 ± 4 nM), while the RFX complex had an affinity comparable to RFX5 alone (K_d = 230 ± 24 nM). When these results are taken together, they indicate that the RFX5 subunit is primarily responsible for X-box DNA recognition.

To test the specificity of DNA binding, the effect of ionic strength on the stability of the protein−DNA interactions was explored. The affinity for RFX binding to the specific HLA DRA X-box oligo was compared to the affinity for RFX binding to a nonspecific oligo, dA·dT (data not shown). To completely abolish the specific binding of RFX to the X-box DNA, concentrations of KCl > 300 mM were required. In contrast, 150 mM KCl was sufficient to eliminate the binding of RFX to the nonspecific dA·dT oligo. These results imply that the purified proteins are competent to recognize and bind their cognate DNA sequences.

RFX Interacts with W-Box DNA Elements. To investigate whether RFX or the individual subunits could interact with the W-box element of the DRA promoter, an oligo containing the W-box sequence was prepared and labeled with fluorescein for use in a fluorescence anisotropy assay. As shown in Figure 7, RFX5 bound to the W box approximately 10-fold weaker than to the X box (K_d = 1.6 ± 0.1 μM). The

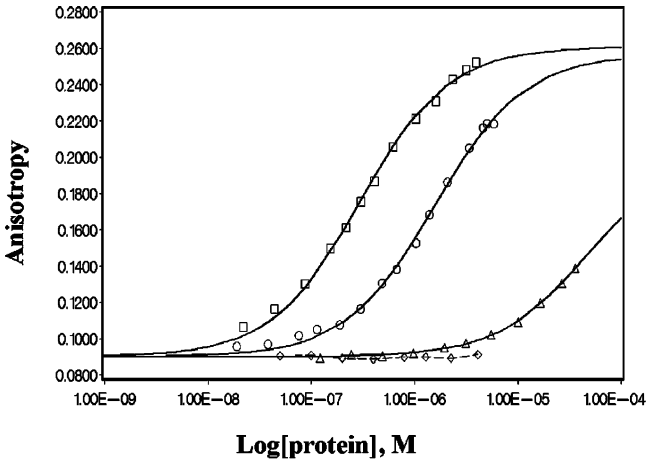

FIGURE 7: Binding of RFX proteins and subcomplexes to W-box DNA. DNA interaction assays were performed using fluorescence anisotropy as described under the Materials and Methods. The fluorescence anisotropy for RFX5 (○), RFX5/RFX-APCA21/FLAG-RFX-ANK (□), RFX-AP (△), and RFX-ANK (◇) was plotted as a function of increasing protein concentration. Nonlinear regression analysis as described under the Materials and Methods converged to the following solutions (where the value in parentheses is the standard error): RFX5, $K_d = 1.6$ (0.13) μM; RFX5/RFX-AP-CA21/FLAG-RFX-ANK, $K_d = 350$ (18) nM.

data suggest a weak interaction between RFX-AP and the W box; however, the relevance and nature of this interaction was not investigated further. RFX-ANK does not bind the W box at the concentrations tested. Interestingly, the trimeric complex of RFX binds to the W box with a higher affinity than that of RFX5 alone ($K_d = 350 \pm 18$ nM), suggesting that the RFX-AP and RFX-ANK subunits enhance the interaction of RFX with the W box of the DRA promoter. Therefore, the purified RFX complex can bind to both the X- and W-box sequences in different ways; binding to the X box occurs with higher affinity and is primarily driven by RFX5, while binding to the W box shows a greater dependence on the RFX-AP and RFX-ANK subunits. The latter interaction may then serve as a scaffold for the addition of other transcription factors to the promoter site.

In Vitro Assembly of the MHC Class II Promoter Complexes. To examine the order of binding and the requirement for DNA in promoter assembly, coprecipitation assays were performed with and without the hybrid oligos mimicking the DRA promoter. Because CIITA binding requires an intact W and X box (*21*, *23*), the DRA W/X box was used for DNA-dependent promoter assembly assays. RFX directly interacts with CIITA in a non-DNA-dependent manner (Figure 8). In fact, CIITA interactions with RFX are diminished in the presence of either specific DNA or nonspecific DNA (oligo dA·dT). Because CIITA has been described as a scaffold protein that facilitates protein−protein interactions to mediate the transcription of MHC class II genes, the loss of CIITA interactions with RFX in the presence of the DRA promoter was unexpected. CREB is pulled down only in the presence of RFX and the specific W/X-box DNA. From these data, we cannot discern whether CREB is pulled down because of an interaction with RFX or based on its interaction with the DNA alone. The faint CREB bands seen in other lanes are the result of a nonspecific interaction with the CA-21 antibody as shown by the fact that a band is detected for CREB alone in the

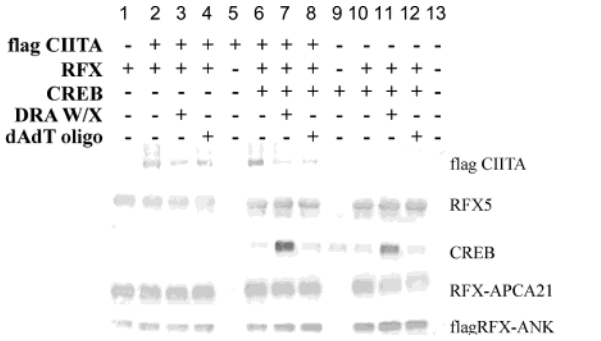

FIGURE 8: Partial assembly of the MHC class II promoter complexes. RFX/CREB, RFX/CIITA, CIITA/CREB, and RFX/CREB/CIITA interactions were examined with and without DNA (either specific W/X box or nonspecific hybrid dA·dT oligo). Anti-CA21 coprecipitation assays were performed by reconstitution of purified transcription factors with and without DNA at a 1:1:1 ratio.

absence of an epitope tag. When these data are taken together, they show that association of CIITA with RFX can occur prior to DNA binding. In the presence of the DRA W/X-box DNA, CIITA binding to RFX is diminished, while CREB binding to RFX appears to be enhanced.

DISCUSSION

The assembly of functional transcription factor complexes on their promoter elements is a multifaceted and poorly understood process. Here, we describe the purification and characterization of several proteins involved in the transcription of MHC class II genes from recombinant baculoviruses. Generation of purified recombinant proteins has allowed for the acquisition of detailed information on the MHC class II transcription factors and their interactions with each other and with DNA.

Using a quantitative fluorescence anisotropy assay, we have demonstrated that RFX5 interacts with the DRA promoter X box with the same affinity as the RFX complex. RFX-AP alone may also bind weakly to DNA as evidenced by our binding curves, but RFX-ANK demonstrates no detectable interaction with DNA. Previous work employing electromobility shift assays using either nuclear extracts or *in vitro* translated transcription factors suggested that only trimeric RFX was competent to bind DNA *(39*−*40*). While it is possible that the other subunits contribute to the stability of the promoter complex *in vivo* or that binding is influenced by the three-dimensional structure of the promoter *in vivo*, our data strongly imply that RFX5 alone is the driving force for recognition of the X box. It is not clear why the recombinant proteins exhibit DNA-binding behavior that is different from proteins obtained from cellular extracts, although the latter may be comprised of phosphorylated species, which could act differently with respect to DNA recognition and promoter assembly. Isolation and biophysical analysis of recombinant versions of the proteins containing the mutations identified in BLS complementation groups B, C, and D may also shed light on the role of the RFX subunits in promoter assembly.

In contrast to the X box, all three subunits were shown to be required for high-affinity binding to the W-box sequence. Although RFX-5 alone binds to the W box ($K_d \approx 2$ μM), the binding affinity is dramatically enhanced in the presence of the RFX-AP and RFX-ANK subunits ($K_d \approx 350$ nM).

Previous studies have demonstrated qualitatively that RFX interacts with the W box, as well as the X box of the DRA promoter *in vivo* (*41*−*42*). Our data provide new evidence that high-affinity recognition of the W box requires the RFX-AP and RFX-ANK subunits of the RFX complex.

Analytical ultracentrifugation studies have provided new insight into the self- and heteroassociation of the RFX subunits, as well as the stoichiometry of the RFX complex. These AUC studies have also elucidated the stoichiometry of the RFX−DNA interaction. Previous published studies have implicated the importance of RFX dimerization for promoter binding. Our data indicate that *in vitro* RFX dimerization is not required for high-affinity recognition of the DRA promoter. Consistent with earlier published electromobility shift assays showing both monomeric and dimeric RFX interacting with the DRA promoter X box (*40*), our data confirm that both monomeric and dimeric forms of RFX5 are competent to bind to the X box. A recent report has suggested that RFX5 proteins unable to form dimers are not capable of supporting MHC class II transcription *in vivo* (*39*). Specifically, a unique dimerization domain within the RFX protein family has been identified by mutational analysis at leucine 66 of the RFX5 protein. Substitution of alanine for leucine at this position resulted in a loss of dimeric DNA binding. Mutation to histidine at this same site was also reported to be responsible for a defect in IFN-γ inducibility, providing a functional link to this leucine-rich motif (62-LYLYQL-68, *43*). The purification schemes provided herein should allow for the isolation of recombinant RFX-5 protein with mutations at these critical sites to further clarify the role of dimerization. One difference between the previous study and this study is the presence of NF-Y, which was shown to interact with RFX5 in cells. The ability of NF-Y and RFX5 to associate may mediate dimerization of RFX5. Clarification of this point will have to wait for the isolation of NF-Y protein and biophysical characterization of its interaction with its binding partners.

The cocrystal structure of the DNA-binding domain of the related RFX1 protein with a symmetrical X-box oligonucleotide duplex revealed two DNA-binding domains bound to opposite sides of the DNA in an antiparallel orientation (*44*). A similar DNA-binding domain (DBD) construct of RFX5 (residues 91−171) was expressed and purified in our laboratory (data not shown). ITC experiments performed with the RFX5-DBD demonstrate a high-affinity interaction with a 1:1 stoichiometry for RFX5-DBD binding to the X box (data not shown). These results suggest that RFX5 recognition of the DRA promoter may occur via a mechanism different from that of RFX1.

Finally, we present coprecipitation data using purified transcription factors, which suggest that the association of CIITA with RFX is not promoter-dependent because these interactions are diminished when the DRA promoter is present. Similarly, the higher order complex of RFX/CREB/CIITA also appears to be altered in the presence of DNA because DNA binding to RFX/CREB hinders the recruitment of CIITA. This DNA-dependent loss of association of CIITA with RFX/CREB was somewhat surprising because previously published results have demonstrated that the presence of CIITA does not affect the stability of the higher order protein complex formed on DNA by RFX, CREB, and NF-Y (*45*). A key distinction between this study and ours is the contribution of NF-Y and the Y box on the promoter assembly, which likely serves to counterbalance the destabilization seen in our system. Evidence to support this interpretation comes from several subsequent reports including the delineation of specific binding interactions between the C-terminal region of RFX5 and NF-Y (*46*). CIITA has also been shown to interact with RFX-ANK and two of the three NF-Y subunits *(47)*. In addition, direct interactions between NF-Y and RFX-ANK *in vitro* have been reported (*39*).

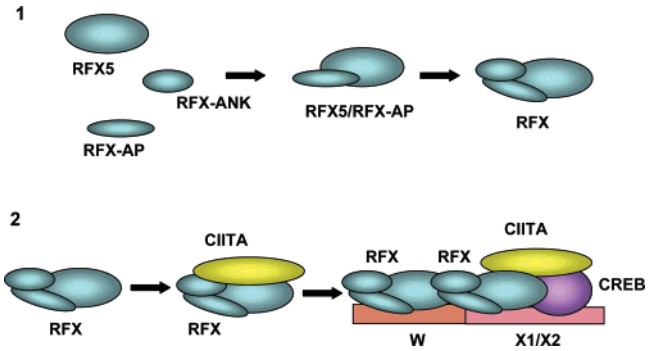

FIGURE 9: Model for assembly of the MHC class II promoter complexes. Scheme 1 depicts the assembly of RFX, with the RFX-AP/RFX5 interaction initiating the formation of the heterotrimer. Interaction between these two subunits results in a conformational change that allows for the recognition of the RFX-ANK subunit. Scheme 2 captures the transcription factor assembly sequence as suggested by our data. RFX and CIITA can preassemble in the absence of DNA. In the presence of W/X-box DRA DNA, the RFX/CIITA interaction is altered (possibly so that CIITA can facilitate the recruitment of additional transcription factors) and RFX/CREB interactions are detected.

In any case, our data suggests a model for promoter assembly, where formation of the RFX heterotrimer is initiated by the RFX5/RFX-AP interaction (Figure 9). This event results in a conformational change that enables RFX-ANK to bind to the subcomplex. This is in contrast to previously published models, which suggest that RFX-5 binds to a preassembled RFX-AP/RFX-ANK complex *(48)*. Recognition of RFX by CIITA occurs in the absence of DNA. In the presence of DNA a conformational change occurs that alters the interaction between CIITA and RFX. The altered interaction between CIITA and RFX within the higher order complex (including CREB) may facilitate recruitment of additional transcription factors, in line with the previously defined role of CIITA as a scaffolding protein.

In conclusion, these studies have biochemically defined each of the RFX proteins that are absolutely necessary for activation of MHC class II gene expression. The intermolecular protein associations within RFX have provided insight into the hierarchy of protein−protein and protein−DNA interactions that regulate the expression of MHC II genes. When these findings are taken together, they suggest a novel model for the assembly of higher order protein complexes prior to DNA binding.

ACKNOWLEDGMENT

The authors gratefully acknowledge Lee Frego for mass spectrometry analysis of the proteins, Maurice Morelock for nonlinear regression analysis of the fluorescence anisotropy data, and Maryanne Brown for critical reading of the manuscript.

REFERENCES

1. Viret, C., and Janeway, C. A. (1999) MHC and T cell development, *Rev. Immunogenet. 1*, 91−104.
2. Cresswell, P. (1994) Assembly, transport, and function of MHC class II molecules, *Annu. Rev. Immunol. 12*, 259−293.
3. Guardiola, J., and Maffei, A. (1993) Control of MHC class II gene expression in autoimmune, infectious, and neoplastic diseases, *Crit. Rev. Immun. 13*, 247−268.
4. Mach, B., Steimle, V., and Reith, W. (1994) MHC class II-deficient combined immunodeficiency: A disease of gene regulation, *Immunol. Rev. 138*, 207−221.
5. DeSandro, A., Nagarajan, U. M., and Boss, J. M. (1999) The bare lymphocyte syndrome: Molecular clues to the transcriptional regulation of major histocompatiblility complex class II genes, *Am. J. Hum. Genet. 65*, 279−286.
6. Mach, B., Steimle, V., Martinez-Soria, E., and Reith, W. (1996) The bare lymphocyte syndrome and the regulation of MHC expression, *Annu. Rev. Immunol. 14*, 301−331.
7. Steimle, V., Otten, L. A., Zuffery, M., and Mach, B. (1993) Complementation cloning of an MHC class II transcativator mutated in hereditary MHC class II deficiency (or bare lymphocyte syndrome), *Cell 75*, 135−146.
8. Durand, B., Kobr, M., Reith, W., and Mach, B. (1994) Functional complementation of major histocompatibility complex class II regulatory mutants by the purified X-box-binding RFX, *Mol. Cell. Biol. 10*, 6839−6847.
9. Steimle, V., Durand, B., Emmanuele, B., Zufferey, M., Hadam, M. R., Mach, B., and Reith, W. (1995) A novel DNA-binding regulatory factor is mutated in primary MHC class II deficiency (bare lymphocyte syndrome), *Genes Dev. 9*, 1021−1032.
10. Durand, B., Sperisen, P., Emeru, P., Barras, E., Zufferey, M., Mach, B., and Reith, W. (1997) RFX-AP a novel subunit of the RFX DNA binding complex is mutated in MHC class II deficiency, *EMBO J. 16*, 1045−1055.
11. Masternak, K., Barras, E., Zufferey, M., Conrad, B., Corhals, G., Aebersold, R., Sanchez, J. C., Hochstrasser, D. F., Mach, B., and Reith, W. (1998) A gene encoding a novel RFX-associated transactivator is mutated in the majority of MHC class II deficiency patients, *Nat. Genet. 20*, 273−277.
12. Nagarajan, U. M., Louis-Plence, P., Desandro, A., Nilsen, R., Bushey, A., and Boss, J. M. (1999) RFX-B is the gene responsible for the most common cause of the bare lymphocyte syndrome a MHC class II immunodeficiency, *Immunity 10*, 153−162.
13. Reith, W., Satola, S., Herreo-Sanchez, C., Amaldi, I., Lisowska-Grospierre, B., Griscelli, C., Hadam, M. R., and Mach, B. (1988) Congenital immunodeficiency with a regulatory defect in MHC class II gene expression lacks a specific HLA-DR promoter binding protein RF-X, *Cell 53*, 897−906.
14. Hooft Van Huijsduijnen, R. A., Bollekens, J., Dorn, A., Benoist, C., and Mathis, D. (1987) Properties of a CCAAT box-binding protein, *Nucleic Acids Res. 15*, 765−7282.
15. Dorn A., Bollekens J., Staub A., Benoist C., and Mathis D. (1987) A multiplicity of CCAAT box-binding proteins, *Cell 50*, 863−872.
16. Hasegawa, S. L., and Boss, J. M. (1991) Two distinct B cell factors bind the HLA-DRA X box region and recognize different subsets of MHC class II promoters, *Nucleic Acids Res. 19*, 6269−6276.
17. Moreno, C. S., Emery, P., Joesph, E. W., Benedicte, D., Reith, W., Mach, B., and Boss, J. (1995) Purified X2 binding protein (X2BP) cooperatively binds the class II MHC X box region in the presence of purified RFX, the X box factor deficient in the bare lymphocyte syndrome, *J. Immunol. 155*, 4313−4321.
18. Moreno, C. S., Rogers, E. M., Brown, J. A., and Boss, J. M. (1997) RFX, a bare lymphocyte syndrome transcription factor is a multimeric phosphoprotein complex, *J. Immunol. 158*, 5841−5848.
19. Vilen, B. J., Cogswell, J. P., and Ting, J. P. (1991) Stereospecific alignment of the X and Y elements is required for major histocompatibility complex class II DRA promoter function, *Mol. Cell. Biol. 11*, 2406−2415.
20. Reith, W., Siegrist, C. A., Durand, B., Barras, E., and Mach, B. (1994) Function of major histocompatibility complex class II promoters requires cooperative binding between factors RFX and NF-Y, *Proc. Natl. Acad. Sci. U.S.A. 91*, 554−558.
21. Masternak, K., Muhlethaler-Mottet, A., Villard, J., Zufferey, M., Steimle, V., and Reith, W. (2000) CIITA is a transcriptional coactivator that is recruited to MHC class II promoters by multiple synergistic interactions with an enhancement complex, *Genes Devel 14*, 1156−1166.
22. Harton, J. and Ting, J. P.-Y. (2000) Class II transactivator: Mastering the art of major histocompatibility complex expression, *Mol. Cell. Biol. 20*, 6185−6194.
23. Zhu, X.-S., Linhoff, M. W., Li, G., Chin, K.-C., Maity, S. N., and Ting, J. P.-Y. (2000) Transcriptional scaffold: CIITA interacts with NF-Y, RFX, and CREB to cause stereospecific regulation of the class II major histocompatibility complex promoter, *Mol. Cell. Biol. 20*, 6051−6061.
24. Steimle, V., Siegrist, C., Mottet, A., Lisowska-Grospierre, B., and Mach, B. (1994) Regulation of MHC class II expression by interferon-γ mediated by the transactivator gene CIITA, *Science 265*, 106−109.
25. Chang, C. H., Fontes, J. D., Peterlin, B. M., and Flavell, R. A. (1994) Class II transactivator (CIITA) is sufficient for the inducible expression of major histocompatability complex class II genes, *J. Exp. Med. 180*, 1367−1374.
26. Mahanta, S. K., Scholl, T., Yang, F. C., and Strominger, J. L. (1997) Transactivation by CIITA the type II bare lymphocyte syndrome-associated factor requires participation of multiple regions of the TATA box binding protein, *Proc. Natl. Acad. Sci. U.S.A. 94*, 6324−6329.
27. Scholl, T., Mahanta, S. K., and Strominger, J. L. (1997) Specific complex formation between the type II bare lymphocyte syndrome-associated transactivators CIITA and RFX5, *Proc. Natl. Acad. Sci. U.S.A. 94*, 6330−6334.
28. Wright, K. L., Chin, K.-C., Linhoff, M., Skinner, C., Brown, J. A., Boss, J. M., Stark, G. R., and Ting, J. P.-Y. (1998) CIITA stimulation of transcription factor binding to major hsitocompatibility complex class II and associated promoters in vivo, *Proc. Natl. Acad. Sci. U.S.A. 95*, 6267−6272.
29. Kara, C. J., and Glimcher, L. H. (1991) In vivo footprinting of MHC class II genes: Bare promoters in the bare lymphocyte syndrome, *Science 252*, 709−712.
30. Kara, C. J., and Glimcher L. H. (1993) Developmental and cytokine-mediated regulation of the MHC class II gene promoter occupancy in vivo, *J. Immunol. 150*, 4934−4942
31. Chin, K.-C., Mao, C., Skinner, C., Riley, J. L., Wright, K. L., and Moreno, C. S., Stark, G. R., Boss, J. M., and Ting J. P.-Y. (1994) Molecular analysis of G1B and G3A INF-γ mutants reveals that defects in CIITA or RFX result in defective class II MHC and II gene induction, *Immunity 1*, 687−697.
32. Pullen, S. S., Miller, H. G., Everdeen, D. S., Dang, T. T.-A., Crute, J. J., and Kehry, M. R. (1989) CD-40-tumor necrosis factor receptor-associated factor (TRAF) interactions: Regulation of CD40 signaling through multiple TRAF binding sites and TRAF hetero-oligomerization, *Biochemistry 37*, 11836−11845.
33. Chin, K.-C., Li, G., and Ting, J. P.-Y. (1997) Importance of acidic, proline/serine/threonine-rich, and GTP-binding regions in the major histocompatibility complex class II transactivator: Generation of transdominant negative mutants, *Proc. Natl. Acad. Sci. U.S.A. 94*, 2510−2506.
34. Dracheva, S., Koonin, E. V., and Crute, J. J. (1995) Identification of the primase active site of the herpes simplex virus type 1 helicase-primase, *J. Biol. Chem. 270*, 14148−14153.
35. Gill, S. C., and Von Hippel, P. H. (1989) Calculation of protein extinction coefficients from amino acid sequence data, *Anal. Biochem. 182*, 319−326.
36. Schuck, P., Perugini, M. A., Gonzales, N. R., Howlett, G. J., and Schubert, D. (2002) Size-distribution analysis of proteins by analytical ultracentrifugation: Strategies and application to model systems, *Biophys. J. 82* (2), 1096−1111.
37. Laue, T. M., Shah, B. D., Ridgeway, T. M., and Pelletier, S. L. (1992) in *Analytical Ultracentrifugation in Biochemistry and Polymer Science* (Harding, S., and Rowe, A., Eds.) pp 90−125, Royal Society of Chemistry, U.K.
38. Hill, J. J., and Royer, C. A. (1997) Fluorescence approaches to study of protein−nucleic acid complexation, *Methods Enzymol. 278*, 390−416.
39. Jabrane-Ferrat, N., Nekrep, N., Tosi, G., Esserman, L. J., and Peterlin, B. M. (2002) Major histocompatibility compatibility complex class II transcriptional platform: Assembly of nuclear factor Y and regulatory factor X (RFX) on DNA requires RFX5 dimers, *Mol. Cell. Biol. 22*, 5616−5625.
40. Reith, W., Herrero-Sanchez, C., Kobr, M., Silacci, P., Berte, C., Barras, E., Fey, S., and Mach, B. (1990) MHC class II regulatory factor RFX has a novel DNA-binding domain and a functionally independent dimerization domain, *Genes Dev. 4*, 1528−1540.

41. Jabrane-Ferrat, N., Fontes, J. D., Boss, J. M., and Peterlin, B. M. (1996) Complex architecture of major histocompatibility complex class II promoters: Reiterated motifs and conserved protein−protein interactions, *Mol. Cell. Biol. 16*, 4683−4690.
42. Fontes, J. D., Jabrane-Ferrat, N., and Peterlin, B. M. (1997) Assembly of functional regulatory complexes on MHC class II promoters in vivo, *J. Mol. Biol. 270*, 336−345.
43. Brickey, W. J., Wright, K. L., Zhu, X. S., and Ting, J. P. (1999) Analysis of the defect in IFN-γ induction of MHC class II genes in G1B cells: Identification of a novel and functionally critical leucine-rich motif (62-LYLYQL-68) in the regulator factor X5 transcription factor, *J. Immunol. 163*, 6622−6630.
44. Gajiwala, K. S., Chen, H., Cornille, F., Roques, B. P., Reith, W., Mach, B., and Burley, S. K. (2000) Structure of the winged-helix protein hRFX1 reveals a new mode of DNA binding, *Nature 403*, 916−921.
45. Villard, J., Muhlethaler-Mottet, A., Bontron, S., Mach, B., and Reith, W. (1999) CIITA-induced occupation of MHC class II promoters is independent of the cooperative stabilization of the promoter-bound multi-protein complexes, *Int. Immunol. 11*, 461−469.
46. Villard, J., Peretti, M., Masternak, K., Barras, E., Caretti, G., Mantovani, R., and Reith, W. (2000) A functionally essential domain of RFX5 mediates activation of a major histocompatibility complex class II promoters by promoting cooperative binding between RFX and NF-Y, *Mol. Cell. Biol. 20*, 3364−3376.
47. Hake, S. B., Masternak, K., Kammerbauer, C., Janzen, C., Reith, W., and Steimle, V. (2000) CIITA leucine-rich repeats control nuclear localization in vivo recruitment to the major histocompatibility complex (MHC) class II enhancesome and MHC class II gene transactivation, *Mol. Cell. Biol. 20*, 7716−7725.
48. Nekrup, N., Fontes, J. D., Geyer, M., and Peterlin, B. M. (2003) When the lymphocyte loses its clothes, *Immunity 18*, 453−457.

BI030262O